Turing patterns on a sphere

C. Varea,[1] J. L. Aragón,[2] and R. A. Barrio[1]
[1]*Instituto de Física, Universidad Nacional Autónoma de México, Apartado Postal 20-364, 01000 México, D.F., Mexico*
[2]*Instituto de Física, Universidad Nacional Autónoma de México, Apartado Postal 1-1010, Querétaro, Qro. 76000, Mexico*
(Received 6 May 1999)

We address the problem of pattern formation on the surface of a sphere using Turing equations. By considering a generic reaction-diffusion model, we numerically investigate the patterns formed under different conditions on the parameter values. Our results show that a closed surface with curvature, as a sphere, imposes geometrical restrictions on the shape of the pattern. This is important in some biological systems where curvature plays an important role in guiding chemical, biochemical, and embryological processes. [S1063-651X(99)02610-0]

PACS number(s): 87.10.+e, 47.54.+r, 05.70.Ln, 82.20.Mj

I. INTRODUCTION

In 1952, Turing settled the basis for explaining biological patterns using two interacting chemicals that, under certain conditions, can generate stable patterns of chemical concentrations from initial near-homogeneity [1]. This phenomenon, termed diffusion-driven instability, has now been shown to occur in chemistry and biology. Experimental results exhibit the formation of striped patterns and spotted patterns, as well as more complicated patterns. Many of these patterns can be reproduced by Turing models, and there is now a vast theoretical and experimental literature in this area (see Maini *et al.* [2] for a review). Reaction-diffusion theory has been used in biological pattern formation by assuming that the nonuniform chemical concentrations arising from diffusion-driven instability act as a prepattern to which cells respond and differentiate accordingly.

Periodic boundary conditions have been universally used since Turing. In previous works [3–5] we studied Turing systems in confined domains and showed that the boundary is important in aligning stripes or orienting triangular lattices of spots in the plane. We also found that the shape of the domain (curvature of the perimeter) turns out to be of importance when modeling the coat pattern of some marine fish, since sources of chemicals that align the pattern are necessary to obtain agreement with the living systems.

However, in spite of recognizing that living fish or other organisms are far from being flat, curvature has been a neglected feature. Its importance was pointed out, almost a century ago, by Thompson in his famous book *On Growth and Form* [6], and currently it is admitted that many chemical and biochemical surface processes are very much dependent on curvature [7]. Notably, we should mention that in 1953 Richards, under direct supervision by Turing, performed some detailed studies of the formation of patterns on spherical surfaces to acomodate the simpler possible patterns found in the monocellular radiolaria [8]. These efforts remained unpublished. More recently, Zykov *et al.* [9] studied the evolution of spiral waves on a spherical surface by numerical integration of a reaction-diffusion system with feedback.

To start examining Turing systems in curved surfaces, we choose to explore pattern formation on the surface of a sphere. This allows us to compare theoretical results with spherical biological systems such as the skeletons of several radiolaria [10–12]. In this work we consider a generic reaction-diffusion model [4] in spherical coordinates, and numerically investigate the patterns formed in different regions of the parameter space.

II. MODEL

Turing systems have the form

$$\frac{\partial \mathbf{U}}{\partial t} = \overline{\mathbf{D}} \nabla^2 \mathbf{U} + \mathbf{F}(\mathbf{U}). \tag{1}$$

These equations describe the dynamical evolution of the concentrations of several chemicals, described by the components of the vector $\mathbf{U}(\overline{x},t)$, at position $\overline{x}$ and time t. The diffusion coefficients are in the matrix $\overline{\mathbf{D}}$, usually chosen to be diagonal with constant elements, and a chemical reaction between the substances is modeled by the (typically nonlinear) functions, $\mathbf{F}=(F_1,F_2,\ldots)$. The review by Maini *et al.* [2] considered the commonly used reaction kinetics, and presented their motivation.

Once the functions $\mathbf{F}$ are specified, the model may contain a set of parameters, and often presents a uniform steady state where all the components of the vector $\mathbf{F}=\mathbf{0}$. This state is unstable under fluctuations within a range of wavelengths. These instabilities are determined by linear analysis for a fixed set of values of the parameters. The instabilities are driven by the diffusion terms, and stabilized by the nonlinear terms producing spatial patterns, as predicted by Turing. This is the now well-known phenomenon of *diffusion-driven instability*.

The above equations are usually solved on some domain $\Omega \subset R^n$ with boundary conditions which may be of Neumann, Dirichlet, Robin, or periodic type. The concentrations of the chemicals are specified at $t=0$, $\forall \overline{x} \in \Omega$.

In many models one considers only the interactions between two chemicals, and the nonlinear functions are usually quadratic or cubic. From Eq. (1) we can derive a simple set of two reaction-diffusion equations by expanding the nonlinear functions around a stationary uniform solution

$(U_1(c),U_2(c))$, given by the zeros of F_1 and F_2, neglecting terms of order higher than cubic (we refer the reader to the paper by Barrio *et al.* [4] for full details, including a linear stability analysis of the resulting equation). The specific forms we shall consider are

$$\frac{\partial u}{\partial t} = D\,\delta\nabla^2 u + \alpha u(1-r_1 v^2) + v(1-r_2 u),$$
$$\frac{\partial v}{\partial t} = \delta\nabla^2 v + \beta v\left(1+\frac{\alpha r_1}{\beta}uv\right) + u(\gamma + r_2 v), \tag{2}$$

where $u = U_1 - U_1(c)$ and $v = U_2 - U_2(c)$, so the uniform stationary solution of Eqs. (2) is the point (0,0). The special arrangement of the parameters α, β, and γ is dictated by conservation relations between chemicals, as explained elsewhere [4], for instance, in order to have only one spatially uniform steady state, $\alpha = -\gamma$. Also, we require the uniform solution to be linearly stable. This will hold for either $\alpha \geqslant 0$ and $\beta \leqslant -\alpha$, or for $\alpha \leqslant 0$ and $\beta \leqslant -1$. The quantity D is the ratio between diffusion coefficients of the two chemicals, which must be different from unity [1], and δ gives the size of the domain in terms of the chosen wavelengths that we want to be present in the patterns. The interaction parameter r_1 is associated with a cubic coupling, and favors the formation of striped patterns. The quadratic coupling r_2 produces spot patterns.

The model equation (2) has proven very useful in understanding the formation of complex Turing patterns in general, and was analyzed in two-dimensional flat domains in Ref. [4]. The model can be easily written in spherical coordinates and solved using a simple Euler method. Linear analysis of this system was carried out following exactly the same method explained and shown in Fig. 1 of Ref. [4], provided that k^2 is interpreted as $l(l+1)/r^2$, where l is the polar index of the spherical harmonics, and r is the radius of the sphere.

III. NUMERICAL CALCULATIONS

To solve Eq. (2), we discretize the Laplacian in spherical coordinates, using a grid with $M \times N$ sites. Therefore, $(\Delta\theta = \pi/M$ and $\Delta\phi = 2\pi/N)$. To avoid the singularity at $\theta = 0$ the grid starts from $\theta = \Delta\theta/2$, so that in the discretized sphere $\theta_m = \Delta\theta/2 + m\Delta\theta$ for $m = 0 \ldots (M-1)$, and $\phi_n = n\Delta\phi$ for $n = 0 \ldots (N-1)$. The sphere is obtained by using boundary conditions such that the missing neighbor of $u(m;n=N-1)$ is $u(m;n=0)$, and the missing neighbor of $u(m=0,M;n=0,\ldots,N/2-1)$ is $u(m=0,M;n=N/2,\ldots,N-1)$. The same procedure is taken with v. Observe that this method is not equivalent to consider the Laplacian on a planar grid with constant intervals, then forming a cube by matching the boundaries, and then inflating the cube, as it has been recently proposed [13]. The fact that the intervals become small near the poles of the sphere produces a very slow convergence of the numerical calculations. However, the presence of the poles is not sensed by the final patterns, as shown below.

In all the calculations we consider a grid of $M = 34$ and $N = 68$, and use a simple Euler method with a time step Δt ranging from 0.001 to 0.003. This value cannot be increased without compromising convergence. As the initial state we consider $u = v = 0$, except on a circle near the equator, where u and v take random values between -0.5 and 0.5.

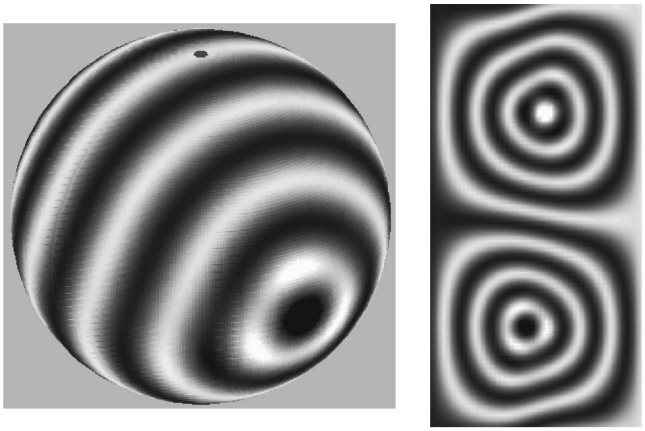

FIG. 1. Pattern of u, drawn with a linear gray scale, obtained after 1 520 000 iterations for $\Delta t = 0.001$ and $\delta = 0.0045$. The other parameters are $r_1 = 3.5$, $r_2 = 0$, $D = 0.516$, $\alpha = 0.899$, $\beta = -0.91$, and $\gamma = -\alpha$. To have a better view of the configuration of stripes, x-y maps of the solutions are also shown, where the horizontal axis corresponds to θ $(0 \leqslant \theta \leqslant \pi)$ and the vertical axis corresponds to ϕ $(0 \leqslant \phi \leqslant 2\pi)$.

We know that the stable patterns can be either spots or stripes, depending on the values of r_1 and r_2. As mentioned above, the quadratic term r_2 favors spots, while the cubic term r_1 produces stripes. Similarly, our extensive numerical simulations suggest that, in general, spots are more robust and that the amplitude differences are larger than those for stripes; that is, spots are more pronounced. The stripes are only formed for very small values of r_2, and can adopt different configurations around the sphere, depending on the initial conditions, and the size of the sphere.

We first consider the formation of striped patterns. It is well known that the sphere cannot be ''combed.'' Therefore, one does not expect a perfect stripped pattern, but there should be at least two defects. These can be point defects, or line defects, as dislocations. If the size of the sphere matches a half-integer number of wavelengths, one obtains closed fringes in the form of rings, that have to end in two opposite spots (defects), whose positions do not necessarily coincide with the geometrical poles of the grid, but depend on the initial conditions. Figure 1 shows an example of this situation.

When this condition is not met, a set of ribbons is obtained. These ribbons are not closed, but have ends on both sides that produce line ''defects'' in the pattern. The particular arrangement of the ribbons around the sphere depends on the size of the system, that is, on δ. As an example of this last situation, in Fig. 2(a) we show a pattern with two black ribbons and one white ribbon; that is, there are four black ends and two white ones. In Fig. 2(b) there is a pattern with only two black defects and two white ones. It seems that this model with only cubic terms does not produce bifurcation of the stripes, typical of labyrinthine patterns in the plane.

Linear analysis [4] allows one to choose the modes that are unstable by tuning D, α, and β. The wavelengths of the unstable eigenmodes are very close to the wavelength stabilized in the nonlinear pattern. Therefore, it is easy to choose

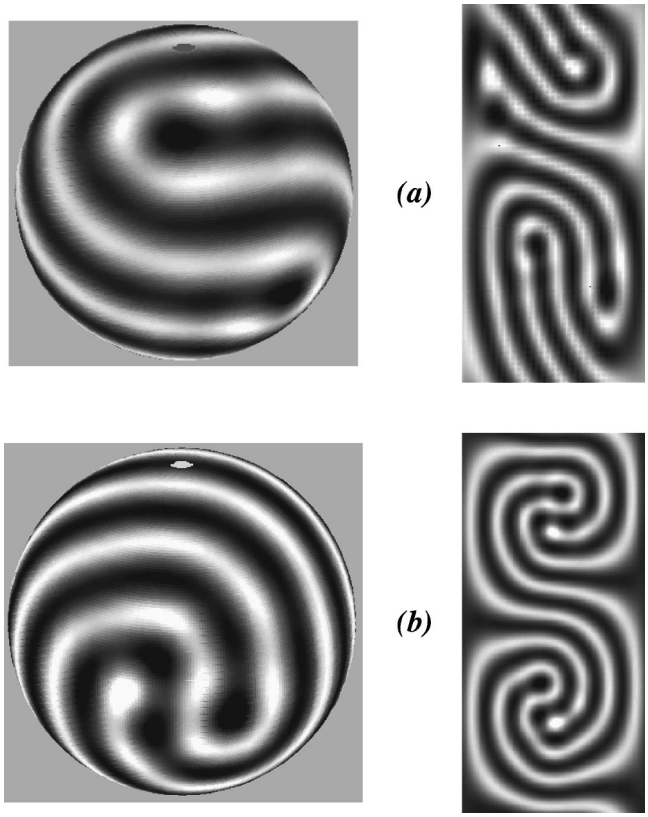

FIG. 2. (a) Pattern of u obtained after 4 800 000 iterations using the same parameters as in Fig. 1, except for $\Delta t=0.003$ and $\delta=0.0029$. (b) Same as (a), but with $\delta=0.0021$.

the system size by changing the value of δ only. In the strip pattern of Fig. 1 the system size was such that an exact number of waves fit on the sphere. This condition to form closed rings is apparently extremely stringent, and one has to use a very small time step to converge to this solution.

Next we consider the formation of spot patterns. We choose $r_1=0.02$ and $r_2=0.2$, as in previous works. The number of spots should be controlled by modifying the system size in terms of the wavelength. First we try to match an integer number of spots on the size of the sphere. As examples, we performed calculations for six, 12, and 20 spots, since regular figures are expected for these numbers.

In Fig. 3 we show a pattern with exactly six stable spots. Observe that the spots are distributed homogeneously on the sphere forming the vertices of a regular octahedron, as shown in the triangular tessellation on the right hand side of the same figure, and where the black spots correspond to maxima of u.

In Fig. 4 we show the pattern with 12 spots, which corresponds to a slightly distorted icosahedron. This distortion can be attributed to a small mismatch in the exact number of wavelengths, since distortions are more visible when one has more spots to accommodate. This difficulty increases when one tries to fit in more spots on the sphere. Also, convergence becomes slower when δ diminishes.

A regular dodecahedron was never obtained. In Fig. 5 a pattern with 20 spots is shown. The tessellation shows vertices with coordinations 6 and 5. The presence of fivefold vertices obeys the fact that the curvature is positive, and Euler's law [14] has to be fulfilled. This is also the reason for

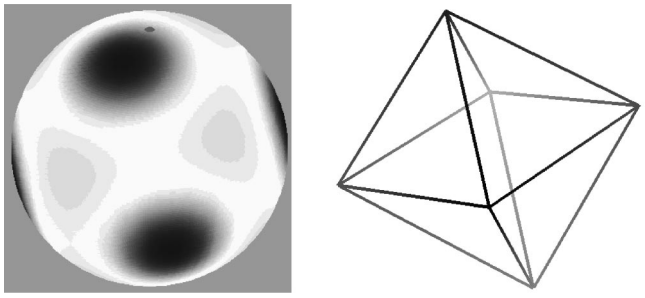

FIG. 3. Pattern with six spots obtained after 250 000 iterations for $r_1=0.02$, $r_2=0.2$, $\Delta t=0.001$, and $\delta=0.0171$. α, β, γ, and D are as in Fig. 1

obtaining triangular lattices in the plane.

In Fig. 6 a pattern with 59 spots is shown. The highly disordered structure with sixfold and fivefold vertices is again the result of the curvature of the sphere. In Fig. 6, all the parameters were changed, because the parameters used in the former figures give spots with radii comparable with the size of the grid.

We observe that when more than 20 spots are involved, the system tends to form structures arranged in a triangular lattice, since the effective curvature is smaller, and the system becomes more planar locally. The proportion of fivefold vertices is a measure of the curvature. Euler proved that the number of elements of any polygonal arrangement has to satisfy the so called Euler's law [14], which in its general form can be written as $F-E+V=\chi$, where F, E, and V are the numbers of faces, edges, and vertices, respectively. In the sphere, the spots can be thought of as being the vertices of imbedded polyhedra. The Euler characteristic χ is a geometric invariant associated with the structure of the same shape or topology. For all polyhedra, $\chi=2$.

For instance, consider a triangular tesselation with only fivefold and sixfold vertices. We know that each face has three edges, and each edge is shared by two faces, thus $F=2E/3$. The number of vertices is the sum of the numbers of the two kinds, $V=N_5+N_6$. Also, the number of edges is $E=(5N_5+6N_6)/2$. Then, according to Euler's law, the number of fivefold vertices is 12 in a closed structure. Therefore if there is a large number of spots, there should be a large number of sixfold vertices, approaching the triangular lattice. The existence of pentagons does not guarantee the sphericity of the closed structure; it can be achieved by introducing defects [15] or distorting the structure. This last situation is mainly what we observe in our calculations when the number of spots increases.

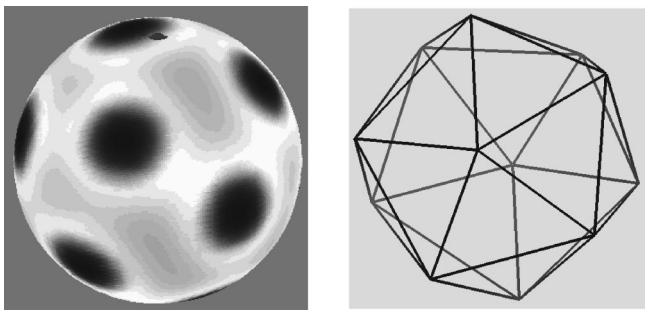

FIG. 4. Pattern with 12 spots obtained after 1 750 000 iterations for $\delta=0.0085$. All the other parameters are as in Fig. 3.

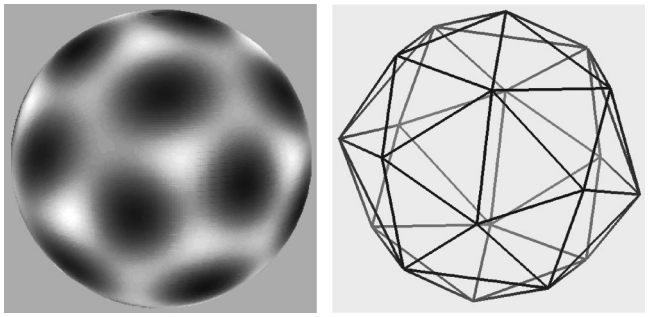

FIG. 5. Pattern with 20 spots obtained after 1 750 000 iterations for $\delta = 0.0045$. All the other parameters are as in Fig. 3.

IV. DISCUSSION AND APPLICATIONS

Turing systems were originally put forward to explain the chemical basis of morphogenesis, that is, how a zygote, which is a spherical object, can acquire a form with a smaller symmetry. Our calculations are ideal to revive this discussion. Very simple unicellular organisms present complicated symmetry breaking that should be compared with Turing's predictions. Among the simplest ones are the *Radiolaria*. These micro-organisms present very beautiful patterns of silicates formed on their membranes. There is an incredible variety of forms, some are spherical and others are conical or elongated. Many, although not all, of the radiolaria skeletons have hexagonal structuring on their surfaces. In Fig. 7 we show photographs of two selected common spherical radiolaria. Notice the resemblance of the skeleton in Fig. 7(a) with our pattern in Fig. 5, and the remarkable correspondence of the skeleton in Fig. 7(b) with our pattern in Fig. 6.

Although the exact process by which these skeletons are formed is not known, we suggest that a simple Turing mechanism, of the sort presented here, might be important as a guide to investigate the chemical oscillations resulting in the final structure. This is matter of other more sophisticated modeling, since it is not clear why SiO_2 is concentrated on the white regions of our diagrams, and how the fibers are stabilized. The biological modelling should be much more laborious.

This work should encourage more reseach on the form of other systems, like viruses. Virus particles also show spherical arrangements with icosahedral symmetry. In Fig. 8 we show some computer graphic representations of viruses as solved by x-ray crystallography [Figs. 8(a) and 8(b)] and by cryoelectron microscopy and image reconstuction [Fig. 8(c)].

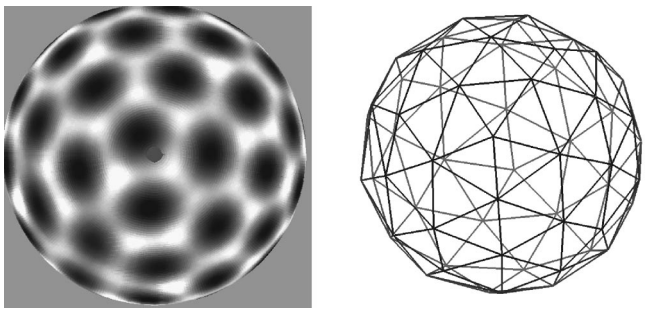

FIG. 6. Pattern with 59 spots obtained after 3 200 000 iterations for $r_1 = 0.02$ and $r_2 = 0.2$. The parameters were $\delta = 0.0074$, $\Delta t = 0.001$, $\alpha = 0.398$, $\beta = -0.4$, and $D = 0.122$.

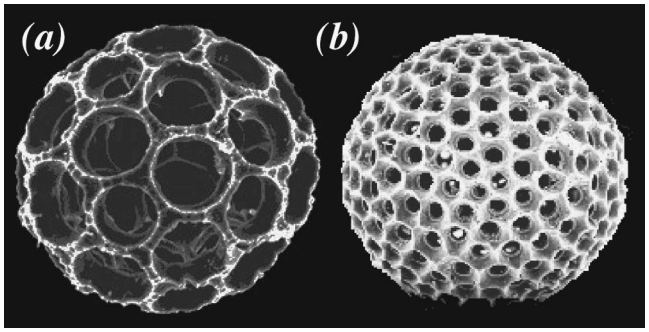

FIG. 7. Silica skeletons of two radiolaria with spherical shape that resemble some of our Turing patterns (reproduced from Ref. [16]).

Notice that the *Bacteriophage Phi X 174* is an icosahedron, and the viruses of Figs. 8(b) and 8(c) show the tendency to form structures arranged in a triangular lattice with some distorted pentagons, as observed in our simulations (Fig. 6).

There are many other examples of systems where patterns are formed on curved surfaces. Lipids, together with proteins, are essential ingredients of all cell membranes and other organelles. Also, pollen grains show a variety of spherical forms with icosahedral polygonal arrangements in the surface. The surface structure of the compound eye of the bumblebee has nearly regular hexagonal faceting upon a segment of spherical surface. These are systems where functionality and curvature are intimately connected [7,12].

We believe that our results constitute a first step toward the exploration of more complex models in non-Euclidean spaces whose importance is being recognized in chemical structures, ranging from atomic and molecular arrangements in crystals, to complex self-assembled colloidal aggregates, and in molecular organization of living systems. Our simulations of spotted patterns can be compared with many biological forms observed in Nature. The skeleton of microscopic sea animals, called Radiolaria, have spherical form with motifs arranged in tetrahedral, octahedral, icosahedral, and other more complex symmetries [6]. Notably, the skeleton of a Radiolarian called *Aulonia hexagona* shows a fairly distorted triangular lattice spread out over the sphere (see Fig. 55 in Ref. [11]). This pattern contains also distorted pentagons as in the example we give in Fig. 6.

Our main conclusion is that curvature is important when investigating the symmetry of Turing patterns. In our model, it seems that stripes tend to be as continuous as possible,

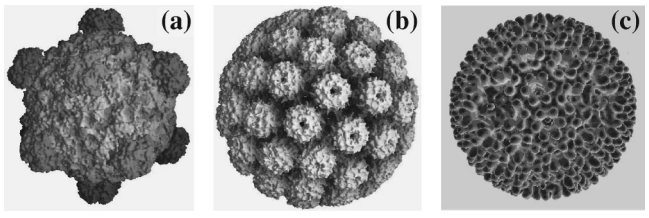

FIG. 8. Computer graphic representation of viruses. (a) Molecular surface of *Bacteriophage Phi X 174* (reproduced from Ref. [17]). (b) Molecular surface of *Simian Virus 40* (reproduced from Ref. [18]). (c) Electron density isosurface of *Mammalian Reovirus Viron* (reproduced from Ref. [19]).

avoiding bifurcactions and presenting a smaller number of defects. In the case where the wavelength matches the size of the system, only two point defects are present, because all the stripes are closed. When spots are formed, they tend to be evenly accommodated, following only geometrical rules that take into account the curvature. In this sense it is not surprising that in a plane only regular triangular lattices are obtained, with only few defects when the initial conditions do not permit orientational matching of the lattice in all the domain (grain boundaries). The existence of grain boundaries on a sphere is not needed. We think this is the reason why micro-organisms that present patterns are so very symmetric.

ACKNOWLEDGMENTS

We want to thank P.K. Maini and H. Terrones for stimulating discussions, and C. Zorrilla for technical aid. Financial support from DGAPA-UNAM through Project Nos. IN-103598, IN-104598, and IN-119698, and from CONACyT through Project Nos. 25237-E and 27643-E is acknowledged. We also thank DGSCA (UNAM) for allowing use of their supercomputing facilities.

[1] A. M. Turing, Philos. Trans. R. Soc. London, Ser. B **237**, 37 (1952).

[2] P. K. Maini, K. J. Painter, and H. N. P. Chau, J. Chem. Soc., Faraday Trans. **93**, 3601 (1997).

[3] C. Varea, J. L. Aragón, and R. A. Barrio, Phys. Rev. E **56**, 1250 (1997).

[4] R. A. Barrio, C. Varea, J. L. Aragón, and P. K. Maini, Bull. Math. Biol. **61**, 483 (1999).

[5] J. L. Aragón, C. Varea, R. A. Barrio, and P. K. Maini, FORMA **13**, 213 (1998).

[6] D'Arcy Thompson, *On Growth and Form*, 2nd ed. (Cambridge University Press, Cambridge, 1968).

[7] S. Hyde, S. Andersson, K. Larsson, Z. Blum, T. Landh, S. Lidin, and B. W. Ninham, *The Language of Shape. The Role of Curvature in Condensed Matter: Physics, Chemistry and Biology* (Elsevier, Amsterdam, 1997).

[8] A. Hodges, *Alan Turing. The Enigma* (Vintage, London, 1983).

[9] V. S. Zykov, A. S. Mikhailov, and S. C. Müller, Phys. Rev. Lett. **78**, 3398 (1997).

[10] R. Williams, *The Geometrical Foundation of Natural Structure* (Dover, New York, 1979).

[11] H. Weyl, *Symmetry* (Princeton University Press, Princeton, 1989).

[12] P. Pearce, *Structure in Nature is a Strategy for Design* (MIT Press, Cambridge, MA, 1978).

[13] M. Taylor, J. Tribbia, and M. Iskandarani, J. Comput. Phys. **130**, 92 (1997).

[14] H. S. M. Coxeter, *Introduction to Geometry* (Wiley, New York, 1989).

[15] M. Terrones and H. Terrones, J. Phys. Chem. Solids **58**, 1789 (1997).

[16] S. Mizutani, Y. Isogai, H. Nagai, and S. Kijima, Rad-File (IDB) Part 1, version 3.68 (29.3 MB, 1498 files), 1997 (unpublished).

[17] R. Mc Kenna, D. Xia, P. Willingmann, L.L. Ilag, and M. G. Rossmann, Acta Crystallogr., Sect. B: Struct. Sci. **48**, 499 (1992).

[18] T. Stehle, S. J. Gamblin, Y. Yan, and S. C. Harrison, Structure **4**, 165 (1996).

[19] K. A. Dryden, G. Wang, M. Yeager, M. L. Nibert, K. M. Coombs, D. B. Furlong, B. N. Fields, and T. S. Baker, J. Cell Biol. **122**, 1023 (1993).